# University of Groningen

## Fetal programming in pregnancy-associated disorders

Stojanovska, Violeta

Publication date:
2018

Link to publication in University of Groningen/UMCG research database

# A double hit preeclampsia model results in sex-specific growth restriction patterns

Violeta Stojanovska
Dorieke J. Dijkstra
Rebekka Vogtmann
Alexandra Gellhaus
Sicco A. Scherjon
Torsten Plösch

**Abstract**

Preeclampsia is a multifactorial pregnancy-associated disorder characterized by an angiogenic dysbalance and systemic inflammation. However, animal models which combine these two pathophysiological conditions are missing. Here we introduce a novel double hit preeclampsia mouse model which mimics the complex multifactorial conditions that are present during preeclampsia and allows the investigation of early consequences for the fetus. Adenoviral overexpression of soluble fms-like tyrosine kinase (sFlt-1) and lipopolysaccharide (LPS) administration at mid-gestation in pregnant mice resulted in hypertension and albuminuria comparable to the manifestation in humans, and more specific for the model we revealed an increased concentration of different types of phosphatidylcholines. The fetuses of both sexes were growth restricted, but only in males, a brain-sparing effect was shown. On the metabolomics levels, male fetuses show changes in the amino acid metabolism, while females showed more pronounced alterations in the lipid metabolism. Our results show that combined exposure to sFlt-1 and LPS mimics the clinical symptoms of preeclampsia *in vivo* and affects fetal growth in a sex-specific manner.

**4**

**Introduction**

Preeclampsia is a multisystemic pregnancy-associated disorder that is identified after the 20th week of gestation with the onset of hypertension and proteinuria [1]. It is the most frequent complication of pregnancy, affecting 3-7% of the population [1,2]. In up to 60% of cases, preeclampsia is further complicated by fetal growth restriction [3,4]. Moreover, preeclampsia and subsequent fetal growth restriction lead to increased susceptibility of the offspring to chronic cardiometabolic diseases in later life (**Chapter 2**). In the recent years, it became apparent that preeclampsia has characteristics of the metabolic syndrome, at least in an altered angiogenic and inflammatory state [6,7].

The concentrations of antiangiogenic factors are elevated in preeclamptic patients [8]; e.g. elevated levels of circulating soluble fms-like tyrosine kinase 1 (sFlt-1) have been shown to be clearly associated with the severity of preeclamptic symptoms [9]. Furthermore, several markers of inflammation are also increased in plasma of preeclamptic patients [10]. Moreover, inflammation impacts the blood pressure and the renal function during pregnancy, contributing to the clinical course of preeclampsia [11,12].

Perturbations in maternal health during pregnancy can lead to morphological and functional changes of major organ systems for life and this has a demonstrable impact on the offspring [13,14]; an effect known as developmental programming. Especially, during early onset preeclampsia there is 2- to 4- fold increased risk of fetal growth restriction [4]. Maladaptation in the fetal autonomic regulation, metabolic and epigenetic changes all have been suggested as a putative predisposing factor in the development of cardiometabolic diseases in growth-restricted offspring [15–17]. However, little is known whether preeclampsia has an effect on the maternal and/or fetal metabolome, which can provide better understanding at the metabolomics level of the relationship between early-life insults and later-life disease susceptibility.

*In vivo* models of preeclampsia are of extreme importance in clarifying the pathophysiological aspects of the disease and in the evaluation of potential fetal programming mechanisms. Inflammatory models of preeclampsia, such as low dose endotoxin infusion [18] or TNFa administration [12], have provided significant insights into kidney and placental pathophysiology during preeclampsia based on inflammatory mechanisms. Furthermore, models that involve antagonism of angiogenesis [19,20] has been widely studied in the evaluation of the maternal and fetal health [21–24]. Altogether, these models are each based only on a single pathophysiological mechanism

[25,26] that results in some of the clinical symptomatology of preeclampsia, not covering the full pathophysiological spectrum that occurs during this disorder. Therefore, we aimed to develop a model that involves the interplay of both antiangiogenesis and inflammation. The current study describes a novel, double hit model of preeclampsia that resembles the complete clinical course in order to investigate the genuine role of antiangiogenesis and inflammation in pregnant mice with regard to metabolic fetal outcomes and function.

### Materials and methods

#### Animals and experimental procedures

C57Bl/6 mice (Charles River, France) between 9-12 weeks old, were housed in a light and temperature controlled facility (lights on from 7:00 am until 7:00 pm, 21 °C). Mouse chow diet (2186 RMH-B, AB diets) and water were provided to the animals ad libitum. Animals were timely mated overnight. The following day the dams were checked for vaginal plug and, if present we counted it as gestational day 0.5 of pregnancy. At gestational day 8.5, animals were randomly assigned to receive either recombinant adenovirus encoding mouse sFlt-1 (Ad-sFlt1) or empty control adenovirus (Adnull) via retroorbital injection. At gestational day 10.5, animals received either 25 ug/kg LPS (E.coli 0111:B4, Sigma-Aldrich, St Louis, MO, USA) in the group that received AdsFlt-1 or PBS (in the group that received the Adnull). At gestational day 16.5, 24 hours urine was collected. At gestational day 18.5, blood pressure was assessed via the abdominal aorta (Datex-Ohmeda, Cardiocap/5). Placenta and fetal tissues were collected at gestational day 18.5. All experiments were approved by the Institutional Animal Care and Use Committee of the University of Groningen (DEC number 6803).

#### Amplification and purification of sFlt-1 and control adenovirus

Adenovirus vector stock of Ad-null (a kind gift from U.J. Tietge, University Medical Center Groningen, the Netherlands) and AdsFlt-1 (a kind gift from S.A. Karumanchi, Beth Israel Deaconess Medical Center, Boston, MA, USA) were used for adenoviral gene delivery. Viruses were amplified in HEK 293A cells at a multiplicity of infection (MOI) of 10. Adenoviral purification was performed with a cesium chloride (CsCl) density gradient (d= 1.45 g/ml and 1,20 g/ml). Adenoviral elution was performed with DG columns (Biorad, Temse, Belgium). The concentration of plaque forming units (PFU) was analyzed with an enzyme-linked immunoassay that detects the adenoviral hexon (Adeasy

viral titer kit, Agilent Technologies, Santa Clara, CA, USA). $1 \times 10^9$ PFU of adenovirus expressing an empty vector (n=9) or mouse sFlt-1 (n=9) in 100 ul PBS were injected via the retroorbital plexus on gestational day 8.5.

**Plasma analysis**

Maternal blood was collected on gestational day 18.5 in EDTA containing tubes (Greiner Bio-One, Kremsmünster, Austria) with heart puncture. Within half an hour the blood was centrifuged for 20 minutes at 1000 rpm and the plasma was stored at -80ºC until analysis. Fetal blood was collected by nicking the left ventricle of the heart, while the fetuses were slightly tilted in order to keep the pooled blood in the thoracic cavity while it was collected in EDTA-coated capillary tubes (Greiner Bio-One, Kremsmünster, Austria). SFlt-1 concentrations in plasma were determined using a mouse sFlt-1 ELISA kit (R&D Systems, Inc., Minneapolis, MN, USA) according to manufacturer's protocol.

**Plasma metabolome detection**

Plasma was obtained and stored as described above. Plasma metabolome analysis was performed with Biocrates AbsoluteIDQ p180 Kit at their facility (Biocrates Life Sciences AG, Austria), as described previously [27]. In short, a commercially available direct flow injection and LC-MS/MS kit was used to analyze 188 available metabolites in plasma samples, including hexose (1), amino acids (21), biogenic amines (21), glycerophospholipids (90), sphingolipids (15) and acylcarnitines (40). Internal standards were pre-pipetted and calibration standard mix in seven different concentrations were included in a standardized assay in 96 well plate format. Per sample 10 ul of plasma was loaded in each well. Derivatization was done with 5% solution of phenyl-isothiocyanate, followed by extraction with addition of methanol with 5 mM ammonium acetate. The samples were delivered to API4000 Qtrap® tandem mass spectrometry instrument (Applied Biosystems, Foste City, CA), using reverse phase HPLC column followed by direct flow injection assay.

**Urine analysis**

Urine samples were collected by placing the pregnant dams in metabolic cages at gestational day 16.5 for 24 hours. The protein and albumin levels were determined using the Pierce BSA Protein Assay Kit (Thermo Fisher Scientific, Rockford, Il, USA) or Assaypro Mouse Albumin Elisa kit (St. Charles, MO, USA), respectively. The concentration of total protein and albumin per sample was multiplied by the 24-hour urine volume.

### Histological analysis

Placenta tissues were fixed in 4% paraformaldehyde (PFA) for 24 hours and stored in 70% ethanol until embedded in paraffin under standard procedures. Placental sections (7 µm) were mounted on standard slides (Engelbrecht Medizin- und Labortechnik GmbH, Edermünde, Germany). For morphological analysis, sections were stained with hematoxylin and eosin (H&E).

### Morphometric analysis

Morphometric analysis of placentae and placental compartments (labyrinth and spongiotrophoblast layer) were performed on nine serial sections of the central region of at least five placentas from each experimental group (control Ad0+PBS, n=5 and AdsFlt+LPS, n=6) with an Axiophot model microscope (Carl Zeiss, Oberkochen, Germany) equipped with a Nikon DS-U1 camera and NIS-BR 3.1 software (Nikon, Düsseldorf, Germany). An auto-white-balance-correction was performed using ImageJ 1.51n (Wayne Rasband, Maryland, USA).

### RNA isolation and gene expression analysis

Total RNA from placentas was extracted with TriReagent (Life Technologies, Carlsblad, CA, USA). RNA quality and quantity was assessed with Nanodrop 2000c (Nanodrop Technologies, Wilmington, DE). cDNA synthesis was performed on 1 µg of total RNA using M-MLV reverse transcriptase (Life technologies, Carlsblad, CA, USA), RNaseOUT (Life Technologies, Carlsblad, CA, USA), random nonamers (Sigma-Aldrich, St Louis, MO, USA). For quantitative real-time PCR, cDNA was amplified with TaqMan (Applied Biosystems, CA, USA) on a StepOnePlus™ Real-Time PCR System (Applied Biosystems, CA, USA). Primers used for RT-qPCR are listed in **supplementary table 1** (see also [28]). The average expression level of mouse beta-actin and GAPDH was used as a house-keeping gene in all qPCR analysis and the standard curve method was used for quantification.

### Statistical analysis

Differences between groups were calculated with the Mann-Whitney U test. Data are presented as median and interquartile range, if not stated otherwise. For all statistical tests, a p-value < 0.05 was considered significant. Pearson R correlation was used to check the association between selected parameters. Data were analyzed using GraphPad Prism 6.0 Software. For metabolomics data, all the analyses were performed with MetaboAnalyst 3.0 [29]. For row-wise normalization we chose to normalize with a reference sample (sample in the control with the least missing values) and column-wise

normalization was done by log2 transformation of the data. Univariate data analysis was performed using volcano plot with fold change threshold of 1.4 and t-tests threshold of 0.1, as well as Mann-Whitney U test. Multivariate data analysis was performed with principal component analysis (PCA) and partial least squares discriminant analysis PLS-DA in order to visualize the metabolic differences between controls and double hit preeclampsia subjects (dam and fetuses). The variable importance in the projection (VIP) scores higher than 1.0 were considered relevant for group discrimination [30].

## Results

### Combined sFlt-1 and LPS exposure induces preeclampsia symptoms in pregnant dams

To study the effects of the proposed model, C57Bl/6 mice were subjected to adenoviral overexpression of sFlt-1, and 48 hours later challenged with LPS. The weight gain, food and water consumption on gestational day 17.5 were not different between the groups (**Supplementary Figure S1B-D**). At gestational day 17.5, total urinary protein excretion (**Supplementary Figure S1A**), as well as of mouse-specific albumin (**Figure 1A**),
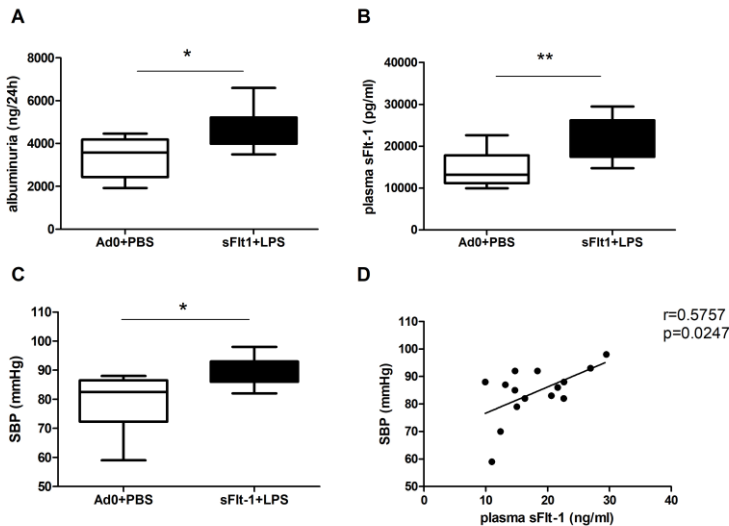


**Figure 1.** Double hit exposure to sFlt-1 and LPS in pregnant dams can induce preeclampsia symptoms. (A) Urine albumin concentration in 24 hour urine samples from pregnant dams at GD 17.5 (n=8-10). (B) Plasma sFlt-1 concentrations from pregnant dams at GD 18.5 (n=8-9).(C) Systolic blood pressure (SBP) in pregnant dams at GD 18.5 (n=7-8). (D) Correlation between sFlt-1 plasma concentrations and systolic blood pressure in pregnant dams (Person r correlation r= 0,57;p= 0,02, n=15). Data are given as median and interquartile range (figure A, B, C), * $p<0.05$; **$p<0.01$.

were significantly increased in the dams that have been exposed to the double hit of sFlt-1 and LPS. In continuation, these dams had 2-fold increased sFlt-1 concentrations in the plasma (**Figure 1B**). On gestational day 18.5, also systolic blood pressure in the pregnant dams exposed to the double hit was significantly increased in comparison to controls (**Figure 1C**). Moreover, there was a positive correlation between the blood pressure values and the obtained sFlt-1 concentrations of the pregnant dams (**Figure 1D**). There were no differences in the number of pups nor in the percentage of resorptions between the groups (**Supplementary Figure S1E, F**). Together, these data show that mid-gestation double hit exposure to sFlt-1 and LPS replicates the clinical features of human preeclampsia in pregnant dams.

**4**

### Clinical features of preeclampsia are not accompanied by changes in placental compartment area

In order to evaluate whether the double hit exposure of pregnant dams to sFlt-1 and LPS differentially affects the placental growth or morphology, we analyzed placental sections at gestational day 18.5. We assessed total placental area as well as different placental compartments, namely the labyrinth and the spongiotrophoblast layer (**Figure 1A**). Total placental area tended to be decreased in the double hit placentas in comparison to controls (**Figure 2B**, p=0.0519). This can be attributed both to the labyrinth and the spongiotrophoblast layer, although the specific changes did not reach statistical significance (**Figure 2C, D**). Assessment of the labyrinth to spongiotrophoblast ratio showed no differences between the double hit placentas and the control ones (**Figure 2E**). Despite the overall decreased placental area, the placental morphology between the double hit preeclamptic dams and controls was unaffected.

### Maternal plasma phosphatidylcholines are increased during double hit preeclampsia

Given that preeclampsia is characterized by widespread adaptations in metabolites [31], including e.g. lipids and carnitines [32] we expected that the double hit preeclamptic dams have a unique metabolomic profile, resembling the human condition. A total of 183 metabolites were investigated by tandem mass (MS/MS) spectrometry. Metabolites that were below the lower limit of quantification (<LLOQ) were excluded; the remaining 141 metabolites were included in the analysis. To identify metabolomic differences between groups, we performed an unsupervised principal component

analysis (PCA) (**Supplementary Figure S2A**) and a supervised partial least squares discriminant analysis (PLS-DA) (**Figure 3A**).
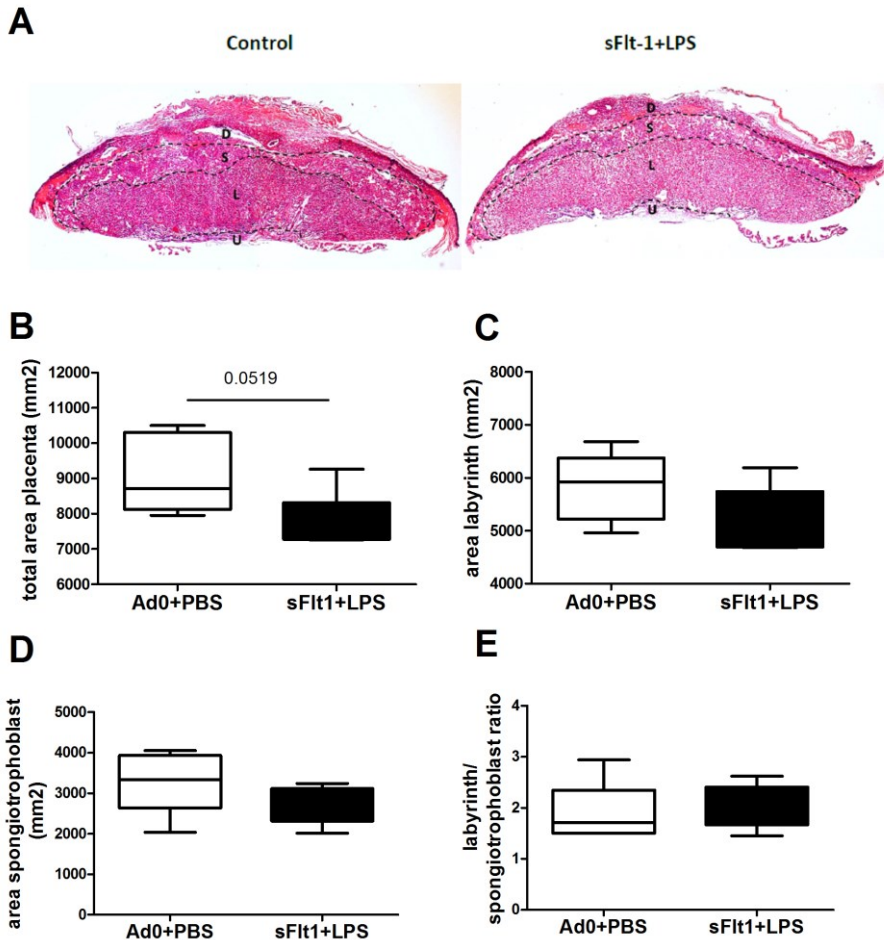


**Figure 2.** Placental morphology at GD 18.5 in double hit preeclampsia model. (A) Placentas were collected and 7 µm sections were stained with hematoxylin and eosin. Scale bar = 1000 µm. D= decidua, S= spongiotrophoblast layer, L= labyrinth layer, U=umbilical cord. Surface area of (B) the whole placenta, (C) the labyrinth layer and (D) the spongiotrophoblast layer were measured in mm². (E) The ratio of the labyrinth area to the spongiotrophoblast area. Data given as mean ± SEM (figure B-E; n=5-6 *p=0,05). Scale bar 1000 µm.
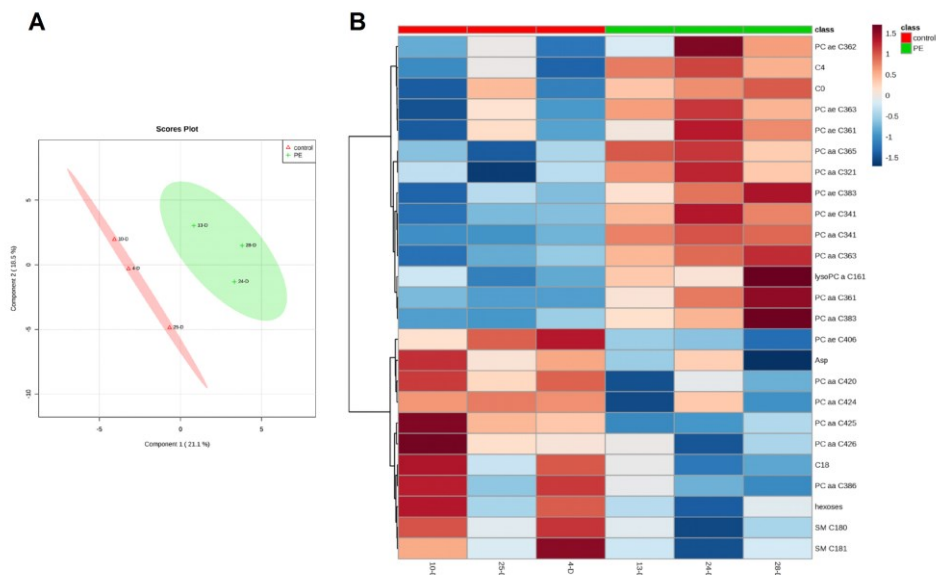
**Figure 3.** Maternal metabolome during double hit preeclampsia (n=3) (A) supervised partial least discriminatory analysis PLS DA on 141 metabolites in plasma of control and double hit PE dams (B) Heat map representation of top 25 modified metabolites, color-coding intensity in the red spectrum shows increase of given metabolites and color intensity in the blue spectrum shows decrease of the given metabolites. Red=Ad0+PBS group, Green=sFlt1+LPS

The results show that the metabolome profile of the double hit preeclamptic dams tends to cluster separately from the one of controls (**Figure 3A**). The clear distinction of these groups is based on the variable importance of projection (VIP) scores obtained from each of the 141 metabolites included in the analysis and the top 15 variable compounds are listed in the **Supplementary Figure S2B**. A heat map representation of the top 25 modified metabolites, showed distinct metabolic footprints between the groups, with the levels of a number of metabolites from the class of phosphatidylcholines (PC) being upregulated in the double hit preeclamptic dams (**Figure 3B**). Furthermore, we examined the top modified metabolites with a threshold combination of fold change and t-tests (p< 0.05). In total, 10 metabolites were significantly changed in the plasma from double hit preeclamptic dams including several long chain fatty acid phosphatidylcholines (PC) and acylcarnitine C4 (**Table 1**).

Table 1. Maternal metabolome during preeclampsia shows increased concentrations majorly in the glycerophosphatydilcholine group of metabolites. FC: fold change; PC-phosphatydilcholine; AA-diacyl; AE-acyl-alkyl; C- carnitine.

| Name | FC | Log2 (FC) | p-value |
|------|-----|-----------|---------|
| PC aa C34:1 | 0.62923 | -0.66834 | 7.0299E-5 |
| PC aa C36:3 | 0.63805 | -0.64825 | 0.0041525 |
| PC ae C34:1 | 0.6201 | -0.68943 | 0.0057079 |
| PC aa C36:5 | 0.50116 | -0.99667 | 0.013278 |
| PC aa C36:1 | 0.55954 | -0.83769 | 0.016105 |
| C4 | 0.47941 | -1.0607 | 0.020592 |
| PC ae C38:3 | 0.61983 | -0.69005 | 0.02596 |
| PC aa C38:3 | 0.51582 | -0.99667 | 0.029883 |
| PC aa C32:1 | 0.51583 | -0.95503 | 0.038355 |
| PC ae C36:3 | 0.56121 | -0.8338 | 0.043259 |

**Fetuses exposed to double hit preeclampsia show growth restriction differences in a sex-specific manner**

Considering that up to 60% of the early onset preeclamptic pregnancies are complicated by fetal growth restriction, we assumed that also our double hit preeclampsia model will lead to impaired fetal growth. Therefore, we phenotyped body size and major organs at GD 18.5 to define the presence and type of growth restriction. Male and female fetuses from double hit preeclamptic dams were lighter in comparison to controls (**Figure 4A**). The liver weight was compromised in both sexes (**Figure 4B**), while the brain was smaller only in the female fetuses that were exposed to double hit preeclampsia (**Figure 4C**). In order to evaluate whether there is a brain sparing effect in our fetuses, we calculated the brain to liver ratio. Brain to liver ratio was significantly increased for the males, while no brain sparing was observed for the females exposed to the double hit preeclampsia (**Figure 4D**). These data show that double hit preeclampsia results in fetal growth restriction and brain sparing is only observed in the males.
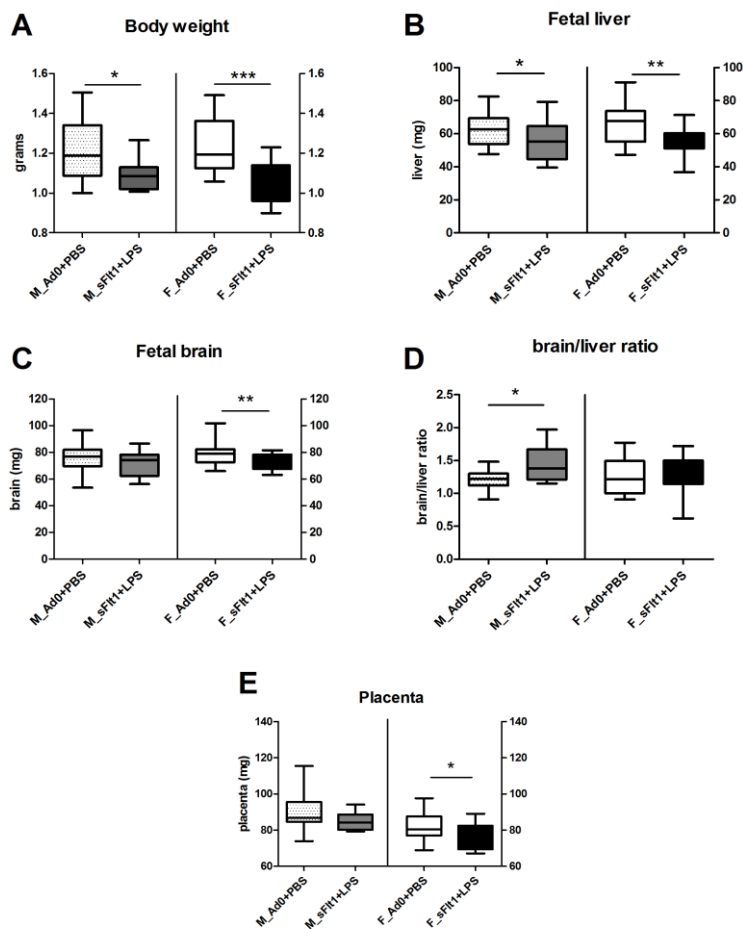
**Figure 4.** Fetal characterization at GD 18 in the double hit preeclampsia model. (A) fetal body weight in grams, (B) fetal liver weight in grams, (C) fetal brain weight in grams, (D) brain to liver ratio, (E) placental weight. All data are given as median and interquartile range, n=17-21, for males and n=18-19 for females; *p<0.05; **p<0.01, ***p<0.001.

### Fetal metabolome after double hit preeclampsia exposure shows sex-specific differences

To explore whether the different growth restriction patterns are associated with metabolomics changes, we analyzed the fetal plasma metabolome. The univariate analysis of log-transformed mouse fetal plasma metabolome data revealed significant

sex-specific differences. The unsupervised principal component analysis (PCA) (**Supplementary Figure S3A**) and the supervised partial least squares discriminant analysis (PLS-DA) (**Figure 5A**) showed an overlap between the metabolic footprint of the



**Figure 5**. Fetal metabolomes are differentially affected by double hit preeclampsia. (A) supervised partial least discriminatory analysis PLS DA on 141 metabolites in plasma of male control fetuses and double hit PE male fetuses, (B) Proline and threonine concentrations in male fetal plasma, (C) supervised partial least discriminatory analysis PLS DA on 141 metabolites in plasma of female control fetuses and double hit PE female fetuses, (D) Plasma concentrations of changed metabolites in female fetal plasma. Data are given as median and interquartile range (figure B,D), n=5 per group, * p<0.05; **p<0.01. Red=Ad0+PBS, green=sFlt1+LPS

males exposed to double hit preeclampsia and the controls. In total only 2 metabolites were significantly decreased in the plasma of the double hit preeclampsia exposed male fetuses when compared to controls, including the amino acids proline and threonine showed significantly reduced levels (p < 0.05) (**Figure 5B**). In comparison, the unsupervised PCA (**Supplementary Figure 3B**) and the supervised PLS-DA)(**Figure 5C**), revealed more obvious clustering pattern between the metabolic footprint of female fetuses exposed to double hit preeclampsia and controls. In total, 5 metabolites showed reduced levels (p<0.05) in the plasma from female fetuses exposed to double hit
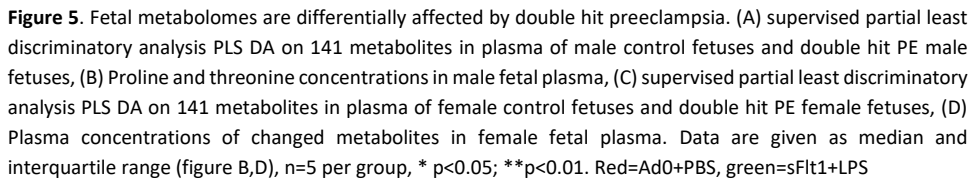
preeclampsia in comparison to controls, including phosphatidylcholines (PC ae 32:1; PC ae 42:1), acylcarnitine (C14:1) and sphingomyelins (SM C24:1; SM C24:0) (**Figure 5D**).

To determine whether these sex-specific metabolomic differences are associated with changes in the placental nutrient transport, we checked the expression levels of several amino acids, fatty acids, and glucose placenta transporters. However, no
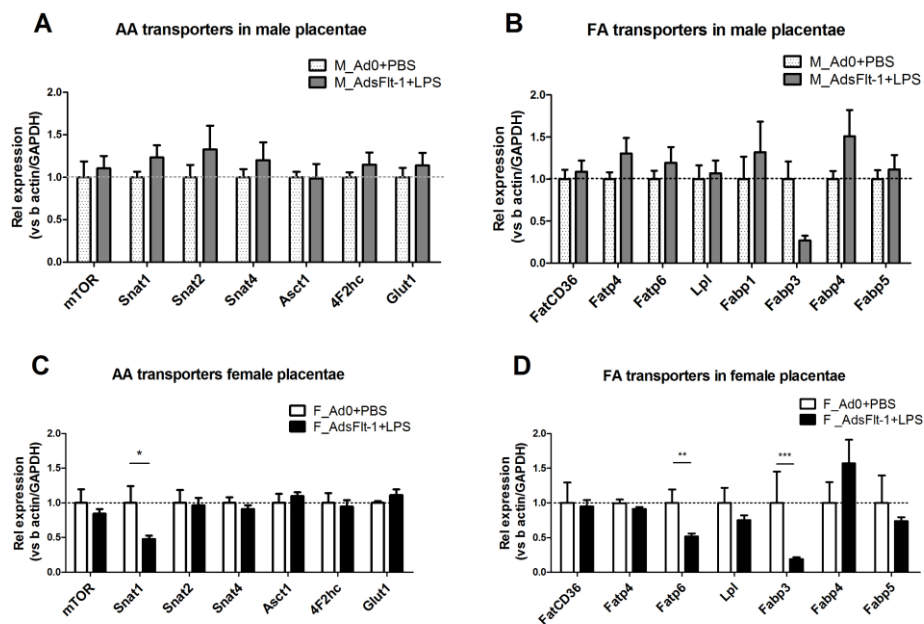


**Figure 6.** Gene expression analysis of important placental nutrient transporters. (A) Amino acid transporters and glucose transporter Glut-1 and (B) fatty acids transporters in male placentas (n=8-9), (C) amino acid transporters and Glut-1 and (D) fatty acid transporters in female placentas. Data given as ± SD;*p<0.5,**p<0.01,***p<0.001.

differences were observed in the gene expression levels between the groups with male placentas (**Figure 6A, B**). In comparison, in the female placentas, there was a significantly decreased expression of sodium-coupled neutral amino acid transporter-1 (Snat-1), fatty acid transporter 6 (Fatp6) and fatty acid binding protein 3 (Fabp3) in the placentas exposed to double hit preeclampsia.

**Discussion**

The results of this study demonstrate that a combined exposure to an antiangiogenic (sFlt-1) and a proinflammatory (LPS) factor leads to preeclampsia in mice, mimicking the characteristics of the disease in human. This double hit exposure leads to smaller placentas, an increase in blood pressure, albuminuria, and increased phosphatidylcholines in the dam. Although the placental compartments were not compromised, fetuses were growth restricted in a sex-specific manner and showed different metabolomic footprints.

Preeclampsia is closely linked to the metabolic syndrome on several levels. Obesity and diabetes mellitus serve as known risk factors for preeclampsia [33,34] and increased pro-inflammatory cytokines contribute to the pathogenesis of preeclampsia [12,35,36]. Furthermore, preeclamptic women are at increased risk to develop cardiovascular diseases in later life [37,38]. Moreover, dysbalance in angiogenesis impacts endothelial function resulting in changes that resemble preeclamptic symptoms, namely by increased plasma sFlt-1 levels and hypertension [19–21]. However, a combined effect of these distinct pathophysiological components to the development of preeclampsia has not been addressed so far. Therefore, a double hit exposure to antiangiogenic factors and low-grade inflammation will be useful in deploying a comprehensive in vivo model for preeclampsia.

Here we reported that exposure to sFlt-1 and LPS in vivo lead to hypertension and albuminuria in the pregnant dam. Although earlier reports suggested that high-dose LPS administration may lead to a fetal loss [39,40], inflammation by means of low dose LPS administration showed no effect on the number of fetuses between the groups in our study. On the other side, the exposure to sFlt-1 antagonize the effect of angiogenic factors such as vascular endothelial growth factor (Vegf) and placental growth factor (Plgf) resulting in endothelial dysfunction [41,42]. With regard to the impact of endothelial dysfunction on blood pressure, it has been previously shown that inhibition of endothelial protectors (such as eNOS) can lead to hypertension [43], granting a role for sFlt-1 in the blood pressure regulation. In our model, we observed increased plasma sFlt-1 levels with a positive correlation with blood pressure values. Altogether, our data suggest that this double hit preeclampsia model is very similar to the human clinical representation of preeclampsia.

4

Studies by Kühnel et al. [28] using a placental-specific overexpression of human sFlt-1 in a lentiviral mouse model of preeclampsia showing placental overexpression of sFlt-1, as one hit, led to IUGR in the fetus and resulted in lower placental weights, the same finding as observed in the double hit model. However, in the study by Kühnel et al. [28] a smaller labyrinth as the transporting trophoblast, and the loss of glycogen cells in the junctional zone could be observed. In contrast to the findings of this study, the expression of the glucose diffusion channel Cx26 is decreased, the expression of one fatty acid transporter, CD36, is significantly increased and the amino acid transporters are unchanged. This differences might be due to the different insults and different mouse strains used in the two mouse models.

Derived from the clinical observation that preeclamptic patients have 4- to 8-fold increased risk to develop cardiovascular disorders in later life [37,38], characterization of their metabolic footprint is of major interest. In preeclampsia, a change in metabolome has been reported [32,44] with specific effects on the fatty acid metabolome, sharing similarities with other cardiovascular and idiopathic inflammatory diseases [45,46]. Moreover, preeclamptic patients show increased choline levels in plasma and urine [47,48] most probably due to increased oxidative stress. In our model, we also report an increase of several types of long-chain fatty acids phosphatidylcholines. This is in agreement with the metabolomics analysis of the transgenic model of preeclampsia employing catechol-O-methyl transferase knockout mice [27]. However, in their model more profound changes were reported in the metabolome including increased levels of several phosphatidylcholines, several sphingomyelins, and acylcarnitines. This can be explained due to model differences, where the latter one acts via inhibition of enzymes involved in the estrogen conversion. Thereby, our intervention with sFlt-1 and LPS only affects the glycerophospholipids metabolites and might contribute to the preeclamptic outcome.

Exposure to a harsh intrauterine environment has been implicated in sex-specific consequences for the offspring in later life [21,49]. Although the relative contribution of sex on the fetal size, body proportions and growth patterns [50] is not well defined, evidence has accumulated that males have increased body weight at birth in comparison to females in uncomplicated pregnancies [51]. In addition, in humans during the first 20 weeks of pregnancy, male fetuses have higher head circumference in comparison to females, but this difference is almost non-existent as the pregnancy prograded [51]. In this context, the timing and exposure to harsh intrauterine stimuli are relevant for sex-

specific outcomes. In the current study, we have shown that exposure to sFlt-1 and LPS during mid-gestational days results in smaller brains in the female fetuses. On the contrary, no weight changes were observed in the male brain, which is consistent with the observation that in humans, males have decreased growth rate of the head circumference in the last weeks of pregnancy [51], making them then less susceptible to the harsh intrauterine conditions. Data on sex-specific differences in the fetal growth responses due to preeclampsia are still limited, but a study from Stark et al reported that female infants have significantly lower birth weight percentiles whereas males maintain normal growth [49]. This is, at least in part, in accordance with our results where female fetuses were also severely affected by symmetrical growth restriction, while on the other hand, males showed brain-sparing and asymmetrical growth restriction.

Sufficient delivery of macronutrients is an important pre-requisite for optimal fetal development. Amino acids, acylcarnitines, and glycerophospholipids act as key metabolic factors for the fetus and the placenta [52]. Moreover, a sudden shift in the source of energy will lead to adaptations in several metabolic processes such as fatty acid oxidation, gluconeogenesis, and ketogenesis [53]. In response to a hypoglycemic insult, several amino acids, including proline and threonine, serve as glucogenic mediators [54]. Furthermore, an excess of stress hormones [55] and inflammatory cytokines [56] can affect the hepatic lipid catabolism and lipid metabolites severely. In our study, we reported that male and female fetuses are affected with different degrees of growth restriction and have differentially affected metabolic profiles. Whereas the males only have lower concentrations of amino acids such as proline and threonine, the females show decreased levels of certain acylcarnitines, sphingomyelins, and glycerophospholipids. This suggests that the symmetrical growth restricted female fetuses in our double hit preeclampsia model have dysbalanced fat and energy metabolism. To our knowledge no metabolomics analysis were previously performed on preeclamptic offspring, however, studies performed on IUGR offspring show that amino acids and carnitine metabolites are the most affected without clear distinction between the sexes.

Finally, it is also possible that alteration of selected transporter genes in the placenta may contribute to the observed growth-restriction phenotype. Interestingly, we registered limited changes in the gene expression pattern of nutrient transporters in the placenta and only decreased levels of amino acid transporter (Snat-1) and fatty acid transporters (Fabp3 and Fatp6) were observed in female placentas exposed to double hit

preeclampsia. In particular, it is known that these fatty acids transporters are increased in obese pregnancies [57], but are quite resilient to hypoxic conditions [58]. Moreover, decreased levels of Snat-1 are associated with growth restriction [59,60] and can be correlated to the severity of the restriction. Our findings that these transporters are down-regulated only in the female double hit preeclamptic placentas suggest that they might be involved in the mechanisms leading to the growth restriction and metabolomic changes. Compatible with this, up-regulation of placental transporters may contribute to fetal overgrowth [61,62]. In contrast, the gene expression was not altered in the male placentas and the minor changes in the metabolic footprint of male fetuses exposed to double hit preeclampsia might be explained by increased fetal or placental consumption of certain metabolites. However, the mechanisms underlying the different metabolomics patterns in fetuses exposed to preeclampsia still remains to be fully elucidated.

**4**

In conclusion, in this study, we present a clinically relevant mouse model that closely mimics human preeclampsia. Moreover, it results in sex-specific differences in the growth restriction pattern and the metabolomics footprint, which in turn can shed a light on the sex-specific programming effect of adult-onset disorders due to preeclampsia.

## References

[1]     Mol BWJ, Roberts CT, Thangaratinam S, Magee LA, De Groot CJM, Hofmeyr GJ. Pre-eclampsia. Lancet 2016; 387:999–1011.

[2]     Rajakumar A, Michael HM, Rajakumar PA, Shibata E, Hubel CA, Ananth Karumanchi S, Thadhani R, Wolf M, Harger G, Markovic N. Extra-placental expression of vascular endothelial growth factor receptor-1, (Flt-1) and soluble Flt-1 (sFlt-1), by peripheral blood mononuclear cells (PBMCs) in normotensive and preeclamptic pregnant women. Placenta 2005; 26:563–573.

[3]     Weiler J, Tong S, Palmer KR. Is fetal growth restriction associated with a more severe maternal phenotype in the setting of early onset pre-eclampsia? a retrospective study. PLoS One 2011; 6:e26937.

[4]     Xiao R, Sorensen TK, Williams WA, Luthy DA. Influence of pre-eclampsia on fetal growth. J Matern Neonatal Med 2003; 13:157–162.

[5]     Stojanovska V, Scherjon SA, Plösch T. Preeclampsia As Modulator of Offspring Health. Biol Reprod 2016; 94:53–53.

[6]     Scioscia M. D-chiro inositol phosphoglycans in preeclampsia: Where are we, where are we going? J Reprod Immunol 2017; 124:1–7.

[7]     Salzer L, Tenenbaum-Gavish K, Hod M. Metabolic disorder of pregnancy (understanding pathophysiology of diabetes and preeclampsia). Best Pract Res Clin Obstet Gynaecol 2015; 29:328–338.

[8]     Hertig A, Berkane N, Lefevre G, Toumi K, Marti HP, Capeau J, Uzan S, Rondeau E. Maternal serum sFlt1 concentration is an early and reliable predictive marker of preeclampsia. Clin Chem 2004; 50:1702–1703.

[9]     Park CW, Joong SP, Shim SS, Jong KJ, Yoon BH, Romero R. An elevated maternal plasma, but not amniotic fluid, soluble fms-like tyrosine kinase-1 (sFlt-1) at the time of mid-trimester genetic amniocentesis is a risk factor for preeclampsia. Am J Obstet Gynecol 2005; 193:984–989.

[10]    Borzychowski AM, Sargent IL, Redman CWG. Inflammation and pre-eclampsia. Semin Fetal Neonatal Med 2006; 11:309–316.

[11]    Kalinderis M, Papanikolaou A, Kalinderi K, Ioannidou E, Giannoulis C, Karagiannis V, Tarlatzis BC. Elevated Serum Levels of Interleukin-6, Interleukin-1β and Human Chorionic Gonadotropin in Pre-eclampsia. Am J Reprod Immunol 2011; 66:468–475.

[12]    Cotechini T, Komisarenko M, Sperou A, Macdonald-Goodfellow S, Adams MA, Graham CH. Inflammation in rat pregnancy inhibits spiral artery remodeling leading to fetal growth restriction and features of preeclampsia. J Exp Med 2014; 211:165–179.

[13]    Davis EF, Newton L, Lewandowski AJ, Lazdam M, Kelly BA, Kyriakou T, Leeson P. Pre-eclampsia and offspring cardiovascular health: mechanistic insights from experimental studies. Clin Sci 2012; 123:53–72.

[14]     Kajantie E, Eriksson JG, Osmond C, Thornburg K, Barker DJP. Pre-eclampsia is associated with increased risk of stroke in the adult offspring the helsinki birth cohort study. Stroke 2009; 40:1176–1180.

[15]     Schäffer L, Müller-Vizentini D, Burkhardt T, Rauh M, Ehlert U, Beinder E. Blunted stress response in small for gestational age neonates. Pediatr Res 2009; 65:231–235.

[16]     Jiménez-Chillarón JC, Díaz R, Martínez D, Pentinat T, Ramón-Krauel M, Ribó S, Plösch T. The role of nutrition on epigenetic modifications and their implications on health. Biochimie 2012; 94:2242–2263.

[17]     Ching T, Ha J, Song MA, Tiirikainen M, Molnar J, Berry MJ, Towner D, Garmire LX. Genome-scale hypomethylation in the cord blood DNAs associated with early onset preeclampsia. Clin Epigenetics 2015; 7:21.

[18]     Faas M, Schuiling G, Baller J, Visscher C, Bakker W. A new model for human preeclampsia. Am J Obstet Gynecol 1994; 171:158–164.

[19]     Maynard SE, Min J, Merchan J, Lim K, Li J, Mondal S, Libermann TA, Morgon JP, Sellke FW, Stillman IE, Epstein FH, Sukhatme VP, et al. Excess placental soluble fms-like tyrosine kinase 1 (sFlt1) may contribute to endothelial dysfunction, hypertension, and proteinuria in preeclampsia. J Clin Invest 2003; 111:649–658.

[20]     Venkatesha S, Toporsian M, Lam C, Hanai J, Mammoto T, Kim YM, Bdolah Y, Lim K-H, Yuan H-T, Libermann TA, Stillman IE, Roberts D, et al. Soluble endoglin contributes to the pathogenesis of preeclampsia. Nat Med 2006; 12:642–649.

[21]     Lu F, Bytautiene E, Tamayo E, Gamble P, Anderson GD, Hankins GD V, Longo M, Saade GR. Gender-specific effect of overexpression of sFlt-1 in pregnant mice on fetal programming of blood pressure in the offspring later in life. Am J Obstet Gynecol 2007; 197:1–5.

[22]     Bytautiene E, Bulayeva N, Bhat G, Li L, Rosenblatt KP, Saade GR. Long-term alterations in maternal plasma proteome after sFlt1-induced preeclampsia in mice. Am J Obstet Gynecol 2013; 208:1–10.

[23]     Bytautiene E, Tamayo E, Kechichian T, Drever N, Gamble P, Hankins GD V, Saade GR. Prepregnancy obesity and sFlt1-induced preeclampsia in mice: Developmental programming model of metabolic syndrome. Am J Obstet Gynecol 2011; 204:398.e1-e8.

[24]     Patten IS, Rana S, Shahul S, Rowe GC, Jang C, Liu L, Hacker MR, Rhee JS, Mitchell J, Mahmood F, Hess P, Farrell C, et al. Cardiac angiogenic imbalance leads to peripartum cardiomyopathy. Nature 2012; 485:333–338.

[25]     McCarthy FP, Kingdom JC, Kenny LC, Walsh SK. Animal models of preeclampsia; Uses and limitations. Placenta 2011; 32:413–419.

[26]     Sunderland N, Hennessy A, Makris A. Animal models of preeclampsia. Am J Reprod Immunol 2011; 65:533–541.

[27]     Stanley JL, Sulek K, Andersson IJ, Davidge ST, Kenny LC, Sibley CP, Mandal R, Wishart DS, Broadhurst DI, Baker PN. Sildenafil Therapy Normalizes the Aberrant Metabolomic Profile in the Comt – / – Mouse

**4**

Model of Preeclampsia / Fetal Growth Restriction. Nat Publ Gr 2015; 5:1–10.

[28] Kuhnel E, Kleff V, Stojanovska V, Kaiser S, Waldschotz R, Herse F, Plosch T, Winterhager E, Gellhaus A. Placental-Specific Overexpression of sFlt-1 Alters Trophoblast Differentiation and Nutrient Transporter Expression in an IUGR Mouse Model. J Cell Biochem 2017; 118:1316–1329.

[29] Xia J, Mandal R, Sinelnikov I V., Broadhurst D, Wishart DS. MetaboAnalyst 2.0-a comprehensive server for metabolomic data analysis. Nucleic Acids Res 2012; 40:127–133.

[30] Jansson J, Willing B, Lucio M, Fekete A, Dicksved J, Halfvarson J, Tysk C, Schmitt-Kopplin P. Metabolomics reveals metabolic biomarkers of Crohn's disease. PLoS One 2009; 4.

[31] Kenny LC, Broadhurst DI, Dunn W, Brown M, North RA, McCowan L, Roberts C, Cooper GJS, Kell DB, Baker PN. Robust early pregnancy prediction of later preeclampsia using metabolomic biomarkers. Hypertension 2010; 56:741–749.

[32] Kelly RS, Giorgio RT, Chawes BL, Palacios NI, Gray KJ, Mirzakhani H, Wu A, Blighe K, Weiss ST, Lasky-Su J. Applications of metabolomics in the study and management of preeclampsia: a review of the literature. Metabolomics 2017; 13:1–20.

[33] Persson M, Cnattingius S, Wikström A-K, Johansson S. Maternal overweight and obesity and risk of pre-eclampsia in women with type 1 diabetes or type 2 diabetes. Diabetologia 2016; 59:2099–2105.

[34] Weissgerber TL, Mudd LM. Preeclampsia and Diabetes. Curr Diab Rep 2015; 15:1–16.

[35] Lockwood CJ, Yen C-F, Basar M, Kayisli UA, Martel M, Buhimschi I, Buhimschi C, Huang SJ, Krikun G, Schatz F. Preeclampsia-related inflammatory cytokines regulate interleukin-6 expression in human decidual cells. Am J Pathol 2008; 172:1571–1579.

[36] Pinheiro MB, Martins-Filho OA, Mota APL, Alpoim PN, Godoi LC, Silveira ACO, Teixeira-Carvalho A, Gomes KB, Dusse LM. Severe preeclampsia goes along with a cytokine network disturbance towards a systemic inflammatory state. Cytokine 2013; 62:165–173.

[37] Irgens HU, Reisaeter L, Irgens LM, Lie RT, Lie RT. Long term mortality of mothers and fathers after pre-eclampsia: population based cohort study. BMJ 2001; 323:1213–7.

[38] Wu P, Haththotuwa R, Kwok CS, Babu A, Kotronias RA, Rushton C, Zaman A, Fryer AA, Kadam U, Chew-Graham CA, Mamas MA. Preeclampsia and future cardiovascular health. Circ Cardiovasc Qual Outcomes 2017; 10:e003497.

[39] Kohmura Y, Kirikae T, Kirikae F, Nakano M, Sato I. Lipopolysaccharide (LPS)-induced intra-uterine fetal death (IUFD) in mice is principally due to maternal cause but not fetal sensitivity to LPS. Microbiol Immunol 2000; 44:897–904.

[40] Silver RM, Edwin SS, Trautman MS, Simmons DL, Branch DW, Dudley DJ, Mitchell MD. Bacterial Lipopolysaccharide-mediated Fetal Death in Murine Decidua in Response to Lipopolysaccharide. J Clin Invest 1995; 95:725–731.

**4**

[41]    Barleon B, Totzke F, Herzog C, Blanke S, Kremmer E, Siemeister G, Marme D, Martiny-Baron G. Mapping of the sites for ligand binding and receptor dimerization at the extracellular domain of the vascular endothelial growth factor receptor FLT-1. J Biol Chem 1997; 272:10382–10388.

[42]    Tsatsaris V, Goffin F, Munaut C, Brichant JF, Pignon MR, Noel A, Schaaps JP, Cabrol D, Frankenne F, Foidart JM. Overexpression of the Soluble Vascular Endothelial Growth Factor Receptor in Preeclamptic Patients: Pathophysiological Consequences. J Clin Endocrinol Metab 2003; 88:5555–5563.

[43]    Sander M, Chavoshan B, Victor RG. A Large Blood Pressure Raising Effect of Nitric Oxide Synthase Inhibition in Humans. Hypertension 1999; 33:937–942.

[44]    Benton SJ, Ly C, Vukovic S, Bainbridge SA. Andree Gruslin award lecture: Metabolomics as an important modality to better understand preeclampsia. Placenta 2017; 60:S32–S40.

[45]    Famularo G, De Simone C, Trinchieri V, Mosca L. Carnitines and its congeners: A metabolic pathway to the regulation of immune response and inflammation. Ann N Y Acad Sci 2004; 1033:132–138.

[46]    Ruiz-Núñez B, Dijck-Brouwer DAJ, Muskiet FAJ. The relation of saturated fatty acids with low-grade inflammation and cardiovascular disease. J Nutr Biochem 2016; 36:1–20.

[47]    Austdal M, Skrastad RB, Gundersen AS, Austgulen R, Iversen AC, Bathen TF. Metabolomic biomarkers in serum and urine in women with preeclampsia. PLoS One 2014; 9:e91923.

[48]    Friesen RW, Novak EM, Hasman D, Innis SM. Relationship of dimethylglycine, choline, and betaine with oxoproline in plasma of pregnant women and their newborn infants. J Nutr 2007; 137:2641–6.

[49]    Stark MJ, Clifton VL, Wright IMR. Neonates born to mothers with preeclampsia exhibit sex-specific alterations in microvascular function. Pediatr Res 2009; 65:291–295.

[50]    Melamed N, Meizner I, Mashiach R, Wiznitzer A, Glezerman M, Yogev Y. Fetal Sex and Intrauterine Growth Patterns. J Ultrasound Med 2013; 32:35–43.

[51]    Broere-Brown ZA, Schalekamp-Timmermans S, Hofman A, Jaddoe WV, Steegers EAP. Fetal sex dependency of maternal vascular adaptation to pregnancy: a prospective population-based cohort study. BJOG 2016; 123:1087–1095.

[52]    Alexandre-Gouabau MC, Courant F, Le Gall G, Moyon T, Darmaun D, Parnet P, Coupé B, Antignac JP. Offspring metabolomic response to maternal protein restriction in a rat model of intrauterine growth restriction (IUGR). J Proteome Res 2011; 10:3292–3302.

[53]    Cotter DG, Ercal B, D'Avignon DA, Dietzen DJ, Crawford PA. Impact of peripheral ketolytic deficiency on hepatic ketogenesis and gluconeogenesis during the transition to birth. J Biol Chem 2013; 288:19739–19749.

[54]    Houin SS, Rozance PJ, Brown LD, Hay WW, Wilkening RB, Thorn SR. Coordinated changes in hepatic amino acid metabolism and endocrine signals support hepatic glucose production during fetal hypoglycemia. Am J Physiol - Endocrinol Metab 2015; 308:E306–E314.

[55]     Rando G, Tan CK, Khaled N, Montagner A, Leuenberger N, Bertrand-Michel J, Paramalingam E, Guillou H, Wahli W. Glucocorticoid receptor-PPARα axis in fetal mouse liver prepares neonates for milk lipid catabolism. Elife 2016; 5:1–31.

[56]     Hashizume M, Yoshida H, Koike N, Suzuki M, Mihara M. Overproduced interleukin 6 decreases blood lipid levels via upregulation of very-low-density lipoprotein receptor. Ann Rheum Dis 2010; 69:741–746.

[57]     Díaz P, Harris J, Rosario FJ, Powell TL, Jansson T. Increased placental fatty acid transporter 6 and binding protein 3 expression and fetal liver lipid accumulation in a mouse model of obesity in pregnancy. Am J Physiol - Regul Integr Comp Physiol 2015; 309:R1569–R1577.

[58]     Jadoon A, Cunningham P, McDermott LC. Regulation of fatty acid binding proteins by hypoxia inducible factors 1a and 2a in the placenta: Relevance to pre-eclampsia. Prostaglandins Leukot Essent Fat Acids 2015; 93:25–29.

[59]     Chen YY, Rosario FJ, Shehab MA, Powell TL, Gupta MB, Jansson T. Increased ubiquitination and reduced plasma membrane trafficking of placental amino acid transporter SNAT-2 in human IUGR. Clin Sci 2015; 129:1131–1141.

[60]     Jansson T, Ylvén K, Wennergren M, Powell TL. Glucose transport and system A activity in syncytiotrophoblast microvillous and basal plasma membranes in intrauterine growth restriction. Placenta 2002; 23:392–399.

[61]     Jansson T, Cetin I, Powell TL, Desoye G, Radaelli T, Ericsson A, Sibley CP. Placental Transport and Metabolism in Fetal Overgrowth - A Workshop Report. Placenta 2006; 27:109–113.

[62]     Segura MT, Demmelmair H, Krauss-Etschmann S, Nathan P, Dehmel S, Padilla MC, Rueda R, Koletzko B, Campoy C. Maternal BMI and gestational diabetes alter placental lipid transporters and fatty acid composition. Placenta 2017; 57:144–151.

**4**

## Supplementary files
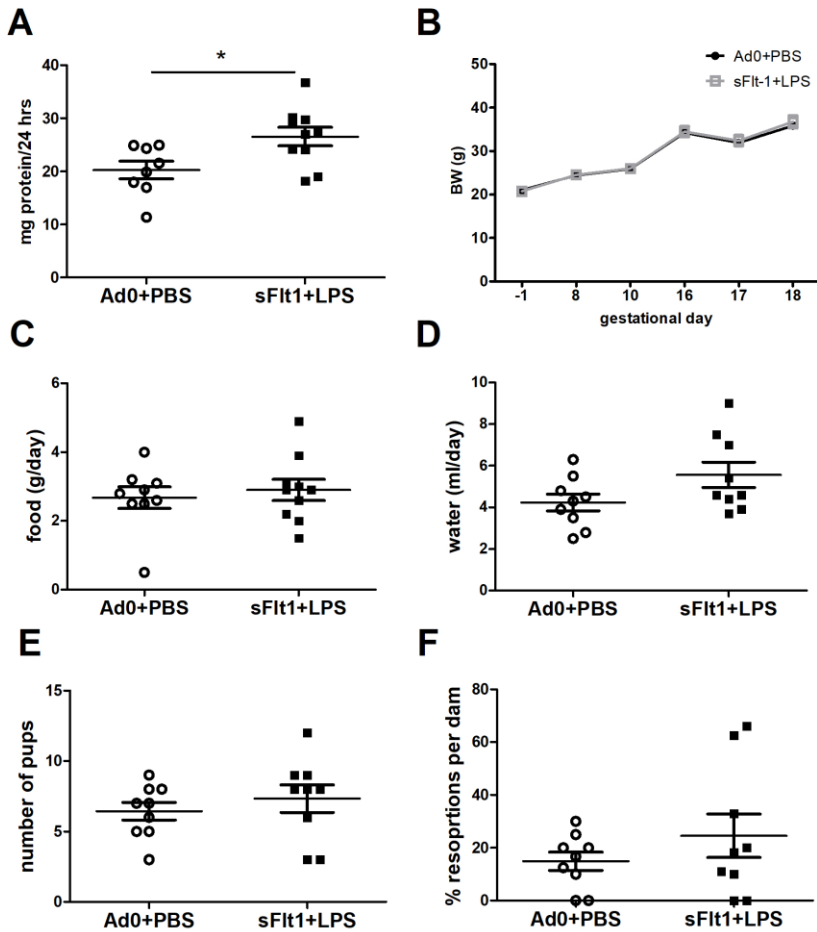


**Supplementary Figure S1.** Maternal characteristics during double hit experimental preeclampsia (A) proteins in 24 hours urine, (B) growth trajectories of pregnant dams, (C) food and (D) water consumption per day for pregnant dams, (D) number of pups and (E) and percentage of resorption per dam. All data are given as ± SEM *p<0.05.
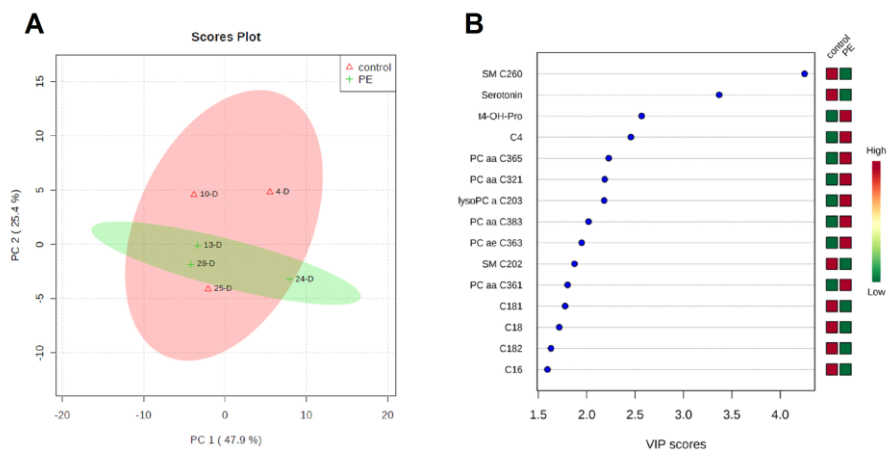
**Supplementary Figure S2.** Metabolome characteristics of the dam (n=3) (A) PCA plot, red=Ad0+PBS; green=sFlt-1+LPS, (B) VIP scores from supervised multivariate analysis of the dam metabolome.
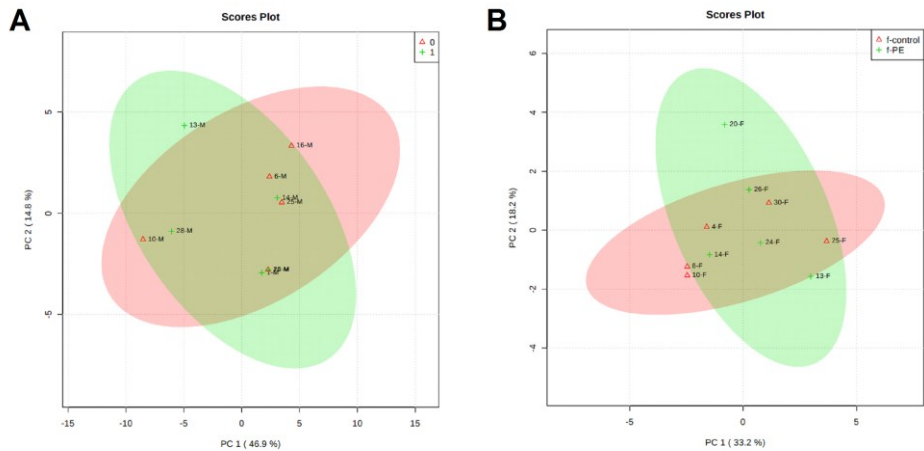


**Supplementary Figure S3.** Metabolome characteristics of male and female fetuses exposed to double hit preeclampsia (A) males principal component analysis PCA plot, (B) females PCA plot.

**Supplementary table 1**. Primer name and primer sequences of different nutrient mouse transporters.

| Primer name | Primer sequence (5' to 3') |
|---|---|
| mTOR forward | GACCTGAGCCGGCAGATTCC |
| mTOR reverse | GTGATCTGCGCAGTGTCGGA |
| Snat1 forward | AGCACAGGCGACATTCTCATC |
| Snat1 reverse | ACAGGTGGAACTTTGTCTTCTTG |
| Snat2 forward | ACAAATGGGTTGTGGTATCTG |
| Snat2 reverse | CCTAGATTTCTCAGCAGTGACAATG |
| Snat4 forward | GGTCTCCCGGTCTAACCCTT |
| Snat4 reverse | AAATTGGCTGTTCATGGCGT |
| Asct1 forward | GGGCCATGTCATCCACGGAG |
| Asct1 reverse | ATGAACACTGCGGCCACACA |
| 4F2hc forward | CAGCGACCTGCTGTTGACCA |
| 4F2hc reverse | GCAGCAGCTGGTAGAGTCGG |
| Glut1 forward | CAACGAGCATCTTCGAGAAGGC |
| Glut1 reverse | CGTCCAGCTCGCTCTACAACAAAC |
| Fat/Cd36 forward | CCAGTGTATATGTAGGCTCATCCA |
| Fat/Cd36 reverse | TGGCCTTACTTGGGATTGG |
| Fatp4 forward | GGCTTCCCTGGTGTACTATGGAT |
| Fatp4 reverse | ACGATGTTTCCTGCTGAGTGGTA |
| Fatp6 forward | GGCTTGAGGATGCCGCTTA |
| Fatp6 reverse | GTACTCTGGGCTCATGCTATGAAGT |
| Lpl forward | AATTTGCTTTCGATGTCTGAGAA |
| Lpl reverse | CAGAGTTTGACCGCCTTCC |
| Fabp1 forward | GTGACTGAACTCAATGGAGACAC |
| Fabp1 reverse | GTAGACAATGTCGCCCAATGTCA |
| Fabp3 forward | CATGAAGTCACTCGGTGTGG |
| Fabp3 reverse | TGCCATGAGTGAGAGTCAGG |
| Fabp4 forward | AAGAAGTGGGAGTGGGCTTT |
| Fabp4 reverse | TCGACTTTCCATCCCACTTC |
| Fabp5 forward | AGAGCACAGTGAAGACGAC |

**4**